ARTICLE

Isoquinolinequinone *N*-oxides as anticancer agents effective against drug resistant cell lines

Received 00th January 20xx,
Accepted 00th January 20xx

DOI: 10.1039/x0xx00000x

Ryan D. Kruschel,[a] Alyah Buzid,[a] Udaya B. Rao Khandavilli,[a] Simon E. Lawrence,[a] Jeremy D. Glennon [a] and Florence O. McCarthy *[a]

The isoquinolinequinone (IQQ) pharmacophore is a privileged framework in known cytotoxic natural product families, caulibugulones and mansouramycins. Exploiting both families as a chemical starting point, we report on the structured development of an IQQ *N*-oxide anticancer framework which exhibits growth inhibition in the nM range across melanoma, ovarian and leukaemia cancer cell lines. A new lead compound (**16**, R6 = benzyl, R7 = H) exhibits nM GI50 values against 31/57 human tumour cell lines screened as part of the NCI60 panel and shows activity against doxorubicin resistant tumour cell lines. An electrochemical study highlights a correlation between electropositivity of the IQQ *N*-oxide framework and cytotoxicity. Adduct binding to sulfur based biological nucleophiles glutathione and cysteine was observed *in vitro*. This new framework possesses significant anticancer potential.

1. Introduction

The quinone moiety is a well-established anticancer framework found in the structures of many broad-spectrum anticancer agents approved by the U.S. Food and Drug Administration (FDA) for clinical use including doxorubicin, daunorubicin, mitomycin C and mitoxantrone. Quinone is a soft electrophile, allowing it to participate in adduct formation *in vivo* to sulfur based nucleophiles including the antioxidant glutathione, amino acid cysteine and DNA which can result in cancer cell death.[1] In addition, redox cycling of the quinone moiety to the semi-quinone radical occurs *in vivo* and is a mechanism of cytotoxicity through generation of Reactive Oxygen Species (ROS) leading to cell cycle arrest and cancer cell death.[2]

The isoquinolinequinone (IQQ) pharmacophore is a privileged framework in known cytotoxic natural product metabolites, caulibugulones and mansouramycins.[3,4] The mansouramycin series comprises of four members originally isolated from marine derived *Streptomyces sp*. (**Figure 1**). Mansouramycins are characterised by having a secondary amine in the C(7) position and differ mainly on the pyridine ring substituents, namely a methyl, ester or indole moiety on C(3) and a methyl or proton on C(4). Analogous to the mansouramycin series the caulibugulone series comprises of six metabolites first isolated from the marine bryozoan *caulibugula intermis*. Caulibugulones A, B, C and D harbour an isoquinolinequinone framework as illustrated in **Figure 1**, whereas caulibugulones E and F comprise of an isoquinolineiminoquinone scaffold. Both natural product series contain halogens as in the case of mansouramycin B and caulibugulone B and C.

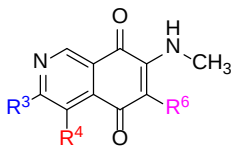

Mansouromycin

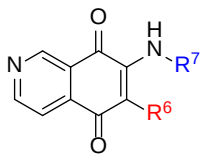

Caulibugulone

	R^3	R^4	R^6
A	CH_3	CH_3	H
B	CH_3	H	Cl
C	$COOCH_3$	H	H
D	Indole	H	H

	R^6	R^7
A	H	CH_3
B	Br	CH_3
C	Cl	CH_3
D	H	EtOH

Figure 1. Structures of known cytotoxic isoquinolinequinone caulibugulones and mansouramycins metabolites.

The mansouramycin family exhibit nM cytotoxicity across multiple cancers including ovarian, breast and melanoma. The most active analogue of the family is mansouramycin C (R^3 = $COOCH_3$) which exhibited an overall potency of 0.089 µM mean IC_{50} value across 36 tumour cell lines in a monolayer cell proliferation assay.[4] In 2017 mansouramycin C was shown to selectively destroy cancer cells in preference to normal human cells through redox cycling mediated ROS generation and subsequent cell death by the opening of the mitochondrial permeability transition pore.[5] In comparison with somatic cells, cancer cells generally experience higher oxidative stress, with an associated increased production of ROS. The introduction of a chemical species which amplifies ROS irreversibly damages the cancer cell leading to cell death. When a somatic cell is exposed to similar ROS augmentation, it is less likely to reach

[a] *School of Chemistry, Analytical and Biological Chemistry Research Facility, University College Cork, Cork T12 K8AF, Ireland; *f.mccarthy@ucc.ie, Tel.: 00353214901695; r.kruschel@umail.ucc.ie*

Electronic Supplementary Information (ESI) available:
See DOI: 10.1039/x0xx00000x

the threshold to trigger cell death due to the reduced basal ROS level.[6]

The caulibugulone series exhibit sub μM IC_{50}'s against murine tumour cell line IC-2^{WT} in an *in vitro* antiproliferative assay.[3] A mechanistic study suggested that caulibugulone A generated modest levels of ROS to irreversibly inhibit Cdc25b leading to cell cycle arrest at the G_1 and G_2/M phases.[7] Overexpression of Cdc25 phosphatases are observed in many cancer types including thyroid, breast, lymphoma and gastric.[8] Interestingly, a similar mechanism of Cdc25 inhibition is suggested for established quinolinequinone based Cdc25 inhibitor, NSC 663284 (**Figure 2**).[9-11]

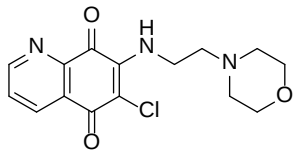

NSC 663284

Figure 2. NSC 663284, an established Cdc25 inhibitor which shares a similar mechanism of action as caulibugulone family

ROS production is heavily entwined in the cytotoxicity of both mansouramycin and caulibugulone (and doxorubicin and quinones in general). Through chemical substitution the quinone can be made increasingly electropositive to more readily undergo redox cycling and become more susceptible to nucleophilic attack by biological nucleophiles.[12-14] Delgado *et al.* identified that addition of an inductively electron withdrawing bromine to the C(6) or C(7) site of IQQs generally result in more cytotoxic derivatives.[15,16] Lending credence, further electrochemical studies suggested that the addition of bromine to the IQQ framework resulted in an increase in redox potential as measured by cyclic voltammetry, corresponding to a more electropositive species.[15, 17]

To date much work has been conducted to explore the chemical space around the IQQ framework to improve anticancer potential using mansouramycin and caulibugulone families as biological starting points. This synthetic work encompasses the amination and thiolation at the C(6) and C(7) positions, halogenation at the C(6) and C(7) positions, amino acid addition to the C(7) and C(6) positions, ring extension and dimer formation.[15-26] Regioselective addition to the quinone moiety remains a problematic issue in current literature. Amination at the C(7) position is predominant in the literature due to regioselective addition of an amine employing cerium chloride as a directing Lewis acid.[20,24]

Herein we report on the expansion of literature knowledge of marine metabolite based isoquinolinequinone generation and their subsequent anticancer screening. We outline the generation of a novel IQQ *N*-oxide framework to probe the ability of the unexplored *N*-oxide moiety to alter the IQQ redox potential allowing the scaffold to possess greater cytotoxicity (**Figure 3**). *N*-Oxides have been employed in drug development and discovered in antitumor natural product alkaloids including calothrixin A.[27,28] The addition of the *N*-oxide has the potential to improve the pharmacological profile through reduction of metabolic oxidation, undergo redox cycling to produce free radicals and hydrogen bond within enzymatic active sites.[29,30] *In silico* correlation studies were conducted employing the NCI60 COMPARE analysis platform to identify a plausible mechanism of action. To confirm activity, adduct binding studies on novel analogues were performed to test their ability to bind to biological nucleophiles *in vitro*.

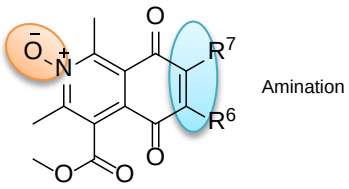

Figure 3. This work describes the effect of *N*-oxide formation to alter the electronics of the quinone to improve its cytotoxicity. Amines are installed at the R^6 and R^7 positions to mimic natural products caulibugulones and mansouramycins.

Results and Discussion

At the outset, the addition of an *N*-oxide moiety to the IQQ framework **2** imbues novelty and is proposed to remove electron density from the system to result in a more redox susceptible electropositive species. We subsequently set out to develop this template.

Development of the Isoquinolinequinone *N*-oxide framework

The IQQ framework **2** was synthesised as a starting point through known literature methodology employing a one-pot silver mediated oxidation/Michael addition (**Scheme 1**).[20] An IQQ *N*-oxide framework **3** was constructed utilising the *m*-CPBA oxidation of **2**. The reaction was high yielding (70%), scalable to multigram quantities and carried out under ambient conditions.

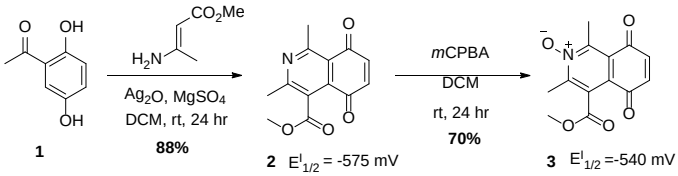

Scheme 1. Synthesis of the IQQ scaffold **2** and its subsequent oxidation with *m*-CPBA resulting in the novel IQQ *N*-oxide framework **3**.

To compare the electrophilicity of IQQ frameworks **2** and **3**, their redox potentials were measured by cyclic voltammetry (CV) in acetonitrile at room temperature using a platinum electrode and 0.1 M tetraethylammonium tetrafluoroborate as the supporting electrolyte and well defined quasi-reversible waves were observed. The first half-wave potentials ($E^I_{1/2}$) related to the formation of the semiquinone radical were evaluated from the resulting voltammograms obtained at a sweep rate of 100 mV s^{-1}.[15,20,31] The redox potential was measured to be -575 mV for IQQ **2**, and -540 mV for IQQ *N*-oxide

3. IQQ *N*-oxide **3** exhibited a more positive redox potential, suggesting it is a more electropositive species.

Regioselective Substitution to IQQ and IQQ *N*-oxide

Taking IQQ **2** and **3** we set out to map the anticancer activity at positions 6 and 7 by amine substitution and halogen incorporation. Methyl, butanol, ethyl morpholine and benzyl amines were chosen based on similarities to known caulibugulones and mansouramycins and to provide chemical diversity. This set of amines were tested on **2** with excellent regioselectivity and moderate to high yields (71-89%) resulting in aminated IQQs **4**-**7** (**Scheme 2**).

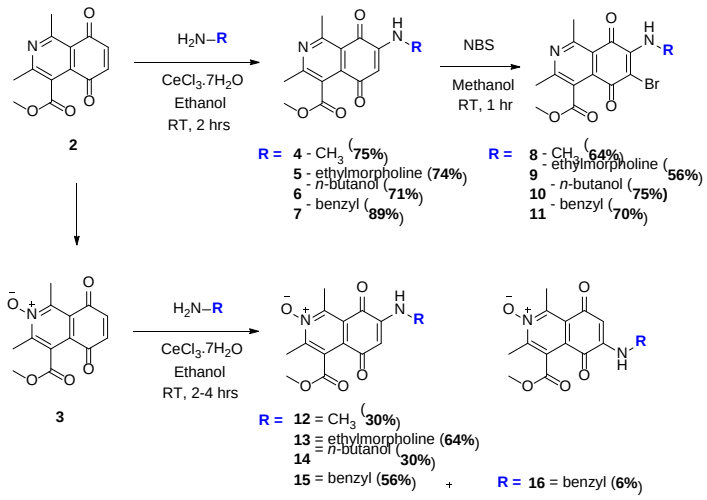

Scheme 2. Regioselective substitution of IQQ framework and generation of fourteen novel analogues

To date regioselective amination to the IQQ scaffold has been inferred by 2D NMR, we present a single crystal X-ray structure of the ethylmorpholino substituted IQQ **5** (**Figure 4**). 2D NMR studies of **5** revealed that the proton at C(6) correlates to C(8) carbonyl carbon (see SI), this is a common trend in the literature often used to confirm whether the C(7) or C(6) isomer is present.[18] Ethyl morpholine IQQ **5** was developed to mimic known quinolinequinone NSC 663284, a potent irreversible inhibitor of Cdc25.

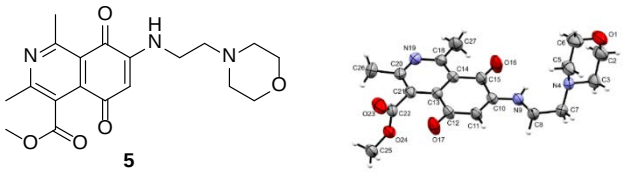

Figure 4. Single crystal X-ray structure of ethyl morpholino isoquinolinequinone **5** confirming C(7) amine addition.

To mimic the natural product caulibugulone B, a bromine was introduced at the C(6) position post-amination employing NBS resulting in analogues **8**-**11** in moderate yields (56-75%). Bromination of the aminated IQQ species has been shown to increase cytotoxicity of the scaffold, partially due to the inductive effect bromine exhibits on the scaffold to make it more redox susceptible.[17]

Utilising the amination procedure as previously described, five IQQ *N*-oxides were furnished **12**-**16** (**Scheme 2**). No evidence of C(6) regioisomer formation was observed after column chromatography for analogues **12**-**14,** however, addition of benzylamine resulted in the formation of two isomers, C(7) aminated **15** and C(6) aminated **16** which were isolated in 56% and 6% yield respectively.

The amination of IQQ *N*-oxide with benzylamine resulted in the generation of two regioisomers. To confirm regioselectivity 2D NMR experiments were performed. Literature precedence for IQQ suggests that the C(5) carbonyl is considered to be more shielded than the C(8) carbonyl.[16,18] For the C(7) benzylamine isomer **15** a three bond correlation of the C(6)H to the more deshielded C(8) carbonyl at 181.1 ppm can be observed (**Figure 5**). For the C(6) benzylamine isomer **16** correlation of the C(7)H to the C(5) carbonyl at 179.1 ppm is noted.

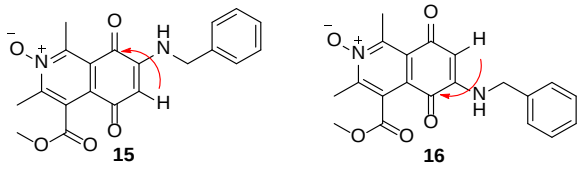

HMBC Correlations (ppm)		
Entry	**^{1}H NMR**	**^{13}C NMR**
15	C6(H) 5.75	C(8) 181.1
16	C7(H) 5.79	C(5) 179.1

Figure 5. HMBC correlations to deduce benzylamine addition site on the IQQ *N*-oxide framework.

Preliminary Cytotoxicity Testing – NCI60 One-Dose Screening

An anticancer *in vitro* assay was conducted in collaboration with the National Cancer Institute 60 human tumour cell lines (NCI60) screening program. The initial methodology involves a one-dose screen at 10 µM concentration across a panel of up to 60 human tumour cell lines.

The aminated IQQ series **4**-**7** exhibited minimal cytotoxicity across most cell lines, the most active being the benzylamine IQQ **7** with a mean tumour cell growth of 82.60% (**Table 1**). The addition of bromine to the IQQ framework significantly improves cytotoxicity across the series with an average 32% decrease in percentage cell growth. The bromo benzyl amine IQQ **11** exhibited potent cytotoxicity against tumour cell lines SK MEL-5, MCF-7, MALME-3M and OVCAR-4 exhibiting percentage cell growths -96.47%, -30.15%, -75.42% and -57.33% respectively.

The IQQ *N*-oxide series **12**-**16** revealed a significantly reduced mean cell growth percentage in comparison to the aminated IQQ series as described in **Table 1**. Looking specifically at the C(6) bromine series **8**-**11** there is similar activity, which supports the *N*-oxide formation increasing the electropositivity

of the quinone, a similar effect observed by Ibacache *et al* through addition of bromine.[17]

Table 1. Preliminary cytotoxic NCI60 one-dose cell growth percentage

Series	Compound	Mean (%) Growth	Growth of selected cell lines (%)					
			MCF-7	COLO-205	MALME-3M	SK MEL-5	OVCAR-3	OVCAR-4
IQQ	**4**	102	95	106	59	84	113	88
6H	**5**	97	81	96	65	86	95	81
	6	91	90	76	67	88	89	86
	7	83	76	79	-2	51	44	65
IQQ	**8**	59	45	31	-27	-91	2	35
6Br	**9**	93	82	56	37	71	13	74
	10	64	38	17	-3	-53	2	38
	11	22	-30	-12	-75	-96	-13	-57
IQQ	**3**	-29	-59	-78	-88	-99	-9	-17
NOX	**12**	61	57	8	-46	-48	7	26
6H	**13**	73	56	7	-13	49	5	35
	14	94	82	60	33	66	71	76
	15	20	-34	-9	-78	-85	1	-79
7H	**16**	-35	-62	-37	-97	-98	-35	-95

Cytotoxic data obtained from the preliminary NCI60 screen. Mean Growth % represents the mean cell growth of 60 cancer cell lines incubated with IQQ analogue at 10μM concentration.

Preliminary cytotoxicity studies on novel IQQ starting scaffold **3** at 10 μM revealed notable cytotoxic activities exhibiting a mean cell growth of -29.45%. The most responsive cancers identified across the series were melanoma (MALME-3M, SK MEL-5), breast (MCF-7), colon (COLO 205) and ovarian (OVCAR-3, OVCAR-4). IQQ *N*-oxide **16** exhibited a lower mean cell growth of -35.10% in comparison to its C(7) regioisomer **15** (19.75%). Compounds which achieve a pre-defined growth inhibition in a minimum number of cell lines progress to five-dose anticancer screening. Four IQQ analogues **3**, **11**, **15** and **16** were advanced to five-dose anticancer screening.

Five-dose Anticancer Screening

Five-dose screening tests active compounds identified from the one-dose screen at 5 concentrations (ranging from 0.01 μM to 100 μM) against the full panel NCI60 cell line panel. The dose-response curve generated enables the determination of three criteria, GI_{50} (drug concentration at which 50% of growth is inhibited), TGI (Total Growth Inhibition) and LC_{50} (drug concentration at which 50% of tumour cells are killed). IQQ's exhibited GI_{50}'s in the sub μM to nM range across multiple cancer cell lines (**Table 2**). The mean GI_{50}'s from the four compounds **3**, **11**, **15** and **16** range from 0.91 μM to 2.93 μM, showing excellent potency. With a mean GI_{50} of 0.91 μM, the C(6) regioisomer **16** is more cytotoxic than the corresponding C(7) isomer **15** (Mean GI_{50} = 2.52 μM) and its's precursor **3** (Mean GI_{50} = 1.75 μM). This is a significant finding with respect to redefining the bioactivity of the isoquinolinequinones.

A full NCI60 five-dose panel trend analysis was conducted using GI_{50} values as illustrated in **Table 3**. Conditional formatting was applied to the GI_{50} values of **3**, **11**, **15** and **16** to visually highlight common responsive cell lines. A high correlation of cancer cell responsiveness can be observed for the IQQ benzylamine analogues **11**, **15** and **16**. The most sensitive tumour cell lines were COLO-205, MALME-3M, OVCAR-3 and OVCAR-4, OVCAR-8, MCF-7, MDA-MB-435 and MDA-MB-468. Interestingly the IQQ *N*-oxide framework **3** did not follow this trend, suggesting it may adopt an alternative or additional mechanism of cytotoxicity.

Table 2. GI_{50}'s of active IQQ benzyl amine analogues across multiple cancer cell lines

Entry	3	11	15	16
Mean GI_{50}	1.75	2.93	2.52	0.91
Mean LC_{50}	28.30	42.14	52.99	23.86

All figures are of μM concentration. Mean GI_{50} was calculated for 53 common human tumour cell lines. Mean LC_{50} was calculated for 50 common cancer cell lines.

Examples of excellent potency are seen for **3** with respect to leukaemia cell line CCRF-CEM, achieving a GI_{50} of 55.9 nM. The most responsive tumour cell lines against **16** were MDA-MB-468 (259 nM), MCF-7 (290 nM), MALME-3M (134 nM), MDA-MB-435 (208 nM), OVCAR-3 (272 nM). The common treatments for OVCAR-3 and OVCAR-4 human cancer cells are the quinone based doxorubicin as well as cisplatin and cyclophosphamide.[32] Responsiveness to quinone based anticancer agents is observed against OVCAR-3 by IQQ's *N*-oxides **3**, **15** and **16** with the most potent being **16**.

IQQ's **3** and **16** also exhibited nM growth inhibition against OVCAR 8 (339 nM and 484 nM respectively), a high grade serous ovarian adenocarcinoma, which has low survival rates.[33] The doxorubicin resistant cell line NCI/ADR-RES is derived from the same individual and shares a large number of karyotypic abnormalities with OVCAR-8. NCI/ADR-RES is less responsive to **3** (2.33μM) but is sensitive to **16** (535 nM). This cell line expresses a high level of multidrug resistance and *P*-glycoprotein, but it is evident that the addition of the benzylamine unit to the 6-position overcomes doxorubicin resistance resulting in a GI_{50} for **16** less than 40 times than that of doxorubicin.[34,35]

The tumour cell lines marked in bold in **Table 3** all harbour the TP53 gene mutation and are responsive in the range of <500 nM.[36] TP53 is a gene which provides instructions to make p53, a critical tumour suppressor and is mutated in approximately 50% of human cancers and has been an attractive target for anticancer agents.[37] There is an obvious correlation between the potency these compounds and the presence of mutant p53.

Redox potential of benzylamine series

The addition of the *N*-oxide moiety to the IQQ benzylamine **7** resulting in **15** results in an enhanced redox ability of the quinone unit observed through an increase in redox potential from -427 mV to -408 mV (**Figure 6**). The C(6) regioisomer **16**

		3	11	15	16
Leukaemia	**CCRF-CEM**	0.0559	3.11	2.98	0.793
	K-562	3.04	3.36	2.94	0.497
	MOLT-4	1.69	3.09	2.21	1.14
	RPMI-8226	2.07	3.24	2.61	1.52
Non-small Cell Lung Cancer	A549/ATCC	3.12	2.56	2.47	1.36
	EKVX	2.02	2.12	2.09	1.18
	HOP-62	0.744	3.12	3.1	1.67
	HOP-92	2.12	2.46	2.8	2.31
	NCI-H226	1.42	4.01	2.81	1.96
	NCI-H23	1.63	1.89	2.03	0.64
	NCI-H322M	1.68	3.45	2.59	1.08
	NCI-H460	2.72	2.94	2.74	0.731
	NCI-H522	1.66	2.25	2.45	1.2
Colon Cancer	**COLO-205**	1.64	1.7	0.977	0.27
	HCC-2998	1.64	3.4	2.8	0.421
	HCT-116	0.945	2.5	2.47	0.305
	HCT-15	1.43	2.76	1.7	0.483
	HT-29	2.41	2.97	1.97	0.374
	KM12	1.99	2.93	2.4	0.653
	SW-620	1.54	3.39	3.12	0.385
CNS Cancer	SF-268	2.05	3.46	2.81	1.48
	SF-295	1.78	3.04	2.6	1.09
	SF-539	1.8	2.85	2.29	1.13
	U251	1.48	2.74	2.46	1.34
Melanoma	LOX IMVI	1.44	2.45	2.72	0.36
	MALME-3M	1.53	1.47	0.617	0.134
	M14	1.78	2.06	1.97	0.729
	MDA-MB-435	1.79	1.86	1.81	0.208
	SK-MEL-2	1.89	2.52	2.63	1.21
	SK-MEL-28	1.96	5.79	4.63	2.21
	SK-MEL-5	1.14	1.47	1.23	0.249
	UACC-257	1.57	1.62	1.7	0.279
	UACC-62	1.63	1.41	1.8	0.316
Ovarian Cancer	IGROV1	1.74	2.05	1.71	0.656
	OVCAR-3	0.314	2.27	0.613	0.272
	OVCAR-4	1.2	1.55	1.13	0.316
	OVCAR-5	1.76	3.11	2.58	1.4
	OVCAR-8	0.339	2.51	2.32	0.484
	NCI-ADR/RES	2.33	2.83	2.67	0.535
Renal Cancer	786-0	2.07	4.65	3.68	2.33
	A498	3.58	4.48	4.72	1.39
	ACHN	1.9	3.08	2.73	1.13
	CAKI-1	1.95	5.66	2.84	0.972
	RXF 393	1.42	3.08	2.47	1.34
	SN12C	1.62	1.49	2.13	0.408
	UO-31	1.69	2.41	2.9	1.26
Prostate	DU-145	1.82	4.26	3.5	1.37
Breast Cancer	MCF7	1.55	1.3	1.65	0.29
	MDA-MB-231/ATCC	2.68	2.11	3.03	0.385
	HS 578T	2.84	10.8	7	1.9
	BT-549	1.72	4.08	4.19	1.49
	T-47D	1.97	2.26	1.88	0.346
	MDA-MB-468	0.946	1.1	1.3	0.259

Table 3. Five-dose GI_{50} trend analysis of **3**, **11**, **15** and **16** against the full panel of human tumour cell lines. Red = most responsive cell lines, Green = least responsive cell line. Values are shown in μM.

exhibits a more positive redox potential of -384 mV when compared to the C(7) isomer **15**, and also exhibits a greater cytotoxicity *in vitro*. A similar observation is made by Delgado *et al.* where an amine at the 7-position of an isoquinolinequinone system has a greater electron donor capacity than an amine at the 6-position, resulting in differences in cytotoxicity.[15]

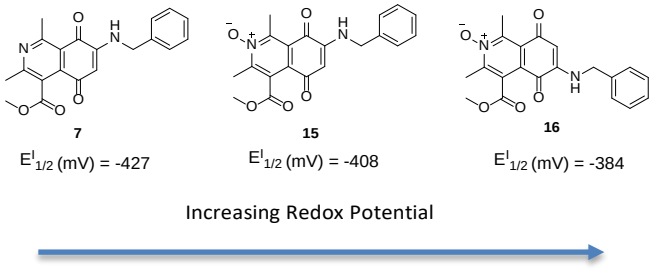

Figure 6. The increasing half-wave potential ($E^{I}_{1/2}$) suggests a correlation to the increase in anticancer activity for **7**, **15** and **16**.

COMPARE Analysis

COMPARE analysis is an *in silico* tool hosted by the National Cancer Institute whose function is to compare useful cytotoxic parameters identified in the five-dose screen such as the GI_{50}, LC_{50} and TGI_{50} of novel analogues against parameters of vast libraries of known anticancer agents to provide insights into possible mechanisms of action. The correlation ranges from 0 (no correlation) to 1 (full correlation). We chose the GI_{50} parameter of the most cytotoxic IQQ *N*-oxides **3**, **15** and **16** for COMPARE analysis (**Table 4**).

The GI_{50} data for IQQ *N*-oxide **3** correlated to antimetabolites 2-deoxyuridine and nelarabine. GI_{50} data from **15** and **16** made significant correlations with many naphthazarin based compounds including (1*S*,3*S*)-austrocortirubin, tetrangulol, NSC 658444 which undergo DNA damage through redox cycling and electrophilic DNA binding (**Figure 7**).[39-42] Due to the similarity of human tumour cell responsiveness of both **15** and **16** as illustrated in **Table 3,** both compounds GI_{50} data correlated reasonably well together with a value of 0.725. In contrast, IQQ's **15** and **16** correlated poorly to **3** as expected, 0.291 and 0.2 respectively.

A direct *in vitro* cytotoxic comparison can be made with the fungal derived (1*S*,3*S*)-austrocortirubin which exhibits a GI_{50} of 3.7 ± 0.6 μM against the human colon cancer cell line HCT116 through inducing DNA damage.[40] IQQ *N*-oxides **15** and **16** exhibit GI_{50}'s of 2.47 μM and 0.305 μM against HCT116 respectively.

Adduct formation studies to probe electrophilicity of Isoquinolinequinone *N*-oxide

As electrophilic species, quinones may be susceptible to glutathione, cysteine and DNA conjugation *in vivo*. A qualitative *in vitro* adduct binding assay was performed to test if binding to amino acids cysteine and serine, and the antioxidant glutathione (**Table 5**) would occur at 37 °C. IQQ **2** and IQQ *N*-oxide **3** formed adducts with all nucleophiles screened. Interestingly upon benzylamine addition **7**, no serine adduct was observed. The IQQ *N*-oxide benzylamine analogues

11,**15**,**16** formed adducts with the thiol-based cysteine and glutathione, again no serine adduct was observed.

Table 4. COMPARE analysis of IQQ *N*-oxides **3**,**15**,**16**

Entry	Correlation	Drug	Mechanism of Action
3	0.711	2-Deoxyuridine	Nucleoside antimetabolite
	0.675	Nelarabine	Purine nucleoside analogue (DNA synthesis inhibition)[38]
15	0.687	Tetrangulol	DNA Intercalation. ROS Production[39]
	0.681	(1*S*,3*S*)-Austrocortirubin	Oxidative Stress (ROS). DNA double strand breaks[40]
	0.653	NSC 331757	Anthraquinone
16	0.725	NSC 658444	DNA Damage. Halting Cell Cycle[41,42]
	0.705	(1*S*,3*S*)-Austrocortirubin	As Above
	0.686	Discorhabdin C-dienol. TFA	Farnesyltransferase enzyme, (HIF-1α), transcriptional co-activator p300 inhibitor[43]
	0.672	NSC 331757	Anthraquinone

Please see supplementary information for drug structures.

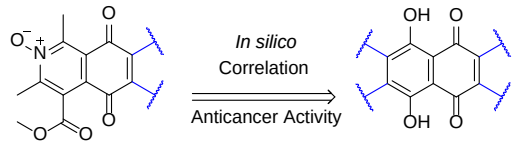

Isoquinolinequinone *N*-oxide Naphthazarin

Figure 7. The highest correlations identified by COMPARE analysis were tetrangulol, (1*S*,3*S*)-austrocortirubin and NSC 658444 which all harbour the naphthazarin framework.

Table 5. Binding IQQ analogues to biological nucleophiles at 37°C

Entry	Adduct Formation		
	Cysteine	Glutathione	Serine
2	✓	✓	✓
3	✓	✓	✓
7	✓	✓	×
11	✓	✓	×
15	✓	✓	×
16	✓	✓	×

✓ = forms adduct, × = no adduct observed. Assay conditions: IQQ (2 mM) incubated with nucleophile (3 mM) in water/methanol at 37°C for 12 hours. The resulting mixture was qualitatively screened using LC/MS for the identification of the adducts. In all cases mono-adduct formation was observed.

Experimental

General Experimental

All solvents were distilled prior to use by the following methods: dichloromethane was distilled from phosphorus pentoxide, ethyl acetate was distilled from potassium carbonate, hexane was distilled prior to use. Organic phases were dried over anhydrous magnesium sulfate. All commercial reagents were procured from both international and local suppliers such as Fluorochem, Acros, Merck and Alpha Aesar and were used without further purification unless stated otherwise. ^{1}H (300 MHz or 400 MHz) and ^{13}C (75 MHz or 100 MHz) NMR spectra were recorded on a Bruker Avance 300 or 400 NMR spectrometer. All spectra were recorded at 20 °C in deuterated dimethylsulfoxide (DMSO- d_6) or deuterated chloroform ($CDCl_3$) using tetramethylsilane (TMS) as an internal standard unless otherwise stated. Chemical shifts (δ_H and δ_C) are reported in parts per million (ppm) relative to the reference peak. The order of citation in parentheses is a) number of protons, b) multiplicity (s =singlet, bs = broad singlet, d = doublet, t = triplet, q = quartet, dd= doublet of doublet, quin. = quintet, sep. = septet, m = multiplet), c) coupling constants, (coupling constants (*J*) are reported in Hertz (Hz)). Infrared spectra were recorded as thin films on sodium chloride plates for oils or as potassium bromide (KBr) discs for solids on a Perkin Elmer Spectrum 100 FT-IR spectrometer or a Perkin Elmer Spectrum One FT-IR spectrometer. Nominal mass spectra were recorded on a Waters Quattro Micro triple quadrupole spectrometer (QAA1202) in ESI mode using 50% acetonitrile – water containing 0.1% formic acid as eluent. High resolution mass spectra (HRMS) were recorded on a Waters LCT Premier Time of Flight spectrometer (KD160) or a Waters Vion IMS mass spectrometer (SAA055K) in ESI mode using 50% acetonitrile – water containing 0.1% formic acid as eluent. Samples (max. 1 mg) were dissolved in acetonitrile, water or 10% DMSO/acetonitrile. Melting points were measured on a uni-melt Thomas Hoover capillary melting point apparatus and are uncorrected. Thin layer chromatography (TLC) was carried out on precoated silica gel plates (Merck 60 PF_{254}). Visualisation was achieved by UV light detection (254 and 366 nm). Wet flash column chromatography was performed using Merck PF_{254} silica gel unless otherwise stated. Single-crystal X-ray analysis was performed on a Bruker APEX II DUO diffractometer at room temperature using graphite monochromatic Mo Kα (λ= 0.7107 Å) radiation. All calculations and refinement were made using the APEX software, containing the SHELX suite of programs[44] and diagrams prepared with Mercury 3.10.[45] All non-hydrogen atoms were located and refined with anisotropic thermal parameters. Hydrogen atoms were included in calculated positions or were located and refined with isotropic thermal parameters.

Methyl 1,3-dimethyl-5,8-dioxo-5,8-dihydroisoquinoline-4-carboxylate (2). A suspension of 2,5-dihydroxyacetophenone (2.040 g, 13.41 mmol), silver(I) oxide (6.081 g, 26.24 mmol), methyl 3-aminocrotonate (1.620 g, 14.07 mmol) and magnesium sulfate (6.405 g) was stirred vigorously at room

temperature in dichloromethane (330 mL) resulting in a black suspension. The reaction mixture was stirred for 18 hours at room temperature until reaction completion, confirmed by TLC (1:1 ethyl acetate: hexane), resulting in a yellow solution with grey precipitate. The entire crude reaction mixture was concentrated under reduced pressure yielding a crude black solid which was subjected to flash column chromatography (9:1 dichloromethane: ethyl acetate) yielding the product as a yellow solid (2.872 g, 88%). m.p. 121.0-123.0 °C (Lit. 120.0 – 122.0 °C); ν_{max}/cm^{-1} (KBr): 3028, 2954, 1726, 1679, 1663, 1568, 1541, 1430, 1383, 1327, 1296, 1254, 1218, 1118, 1090, 871; δ_H (300 MHz, $CDCl_3$): 2.62 [3H, s, C(3)CH_3], 2.97 [3H, s, C(1)CH_3], 4.02 [3H, s, COO(CH_3)], 6.95 [2H, s, C(6,7)CH]; m/z (ESI^+): 246.2 $(M+H)^+$, 100%.

4-(Methoxycarbonyl)-1,3-dimethyl-5,8-dioxo-5,8-dihydroisoquinoline 2-oxide (3). Methyl 1,3-dimethyl-5,8-dioxo-5,8-dihydro-isoquinoline-4-carboxylate (0.211 g, 0.860 mmol) was dissolved in dichloromethane (3 mL) with stirring resulting in a dark yellow solution. *meta*-Chloroperoxybenzoic acid (0.282 g, 1.634 mmol) was then added resulting in a transparent orange solution. The reaction was stirred at room temperature for 24 hours resulting in a dark orange solution with white precipitate. TLC analysis was undertaken at this point to ensure reaction completion (1:1 ethyl acetate: hexane). The entire reaction mixture was concentrated under reduced pressure yielding a crude orange solid. Column chromatography was performed on this crude material (0:1 ethyl acetate: hexane – 3:7 ethyl acetate: hexane) yielding the product as an orange solid, (0.150 g, 70%). m.p. 119.0 – 120.0 °C (degradation); ν_{max}/cm^{-1} (KBr): 3069, 2952, 1743, 1662, 1436, 1375, 1331, 1299, 1231, 1064, 853; δ_H (400 MHz, $CDCl_3$): 2.52 [3H, s, C(3)CH_3], 2.97 [3H, s, C(1)CH_3], 4.04 [3H, s, COO(CH_3)], 6.97 [2H, d, *J* = 3.8 C(6,7)CH]; δ_C (100 MHz, $CDCl_3$): 14.7, 16.2, 53.5, 122.2, 124.9, 128.2, 137.3, 139.9, 151.0, 152.1, 166.2, 181.7, 184.3; m/z (ESI^+): 262.2 $(M+H)^+$, 100%, HRMS (ESI^+): Exact mass calculated for $C_{13}H_{12}NO_5$ 262.0715. Found 262.0705.

Typical procedure for amination

A suspension of isoquinolinequinone (1 equivalent), cerium chloride heptahydrate (spatula tip, catalytic), 4-(2-aminoethyl)morpholine (2 equivalents) in absolute ethanol (30 mL) was stirred for 3-6 hours at room temperature. The consumption of the isoquinolinequinone was monitored using TLC. The reaction mixture was then concentrated under reduced pressure and was subjected to flash column chromatography (ethyl acetate: hexane). The product was isolated and was dried overnight under reduced pressure. An ethyl acetate/hexane recrystallisation was required on analogue **6** to form a solid.

Methyl-1,3-dimethyl-7-(methylamino)-5,8-dioxo-5,8-dihydroisoquinoline-4-carboxylate (4). Amination methyl 1,3-dimethyl-5,8-dioxo-5,8-dihydroisoquinoline-4-carboxylate (0.487 g, 1.99 mmol), by methylamine (33% solution in absolute ethanol) (0.51 mL, 4.10 mmol) yielding the product as a red solid, (0.407 g, 75%). m.p. 268.0 – 270.0 °C; ν_{max}/cm^{-1} (KBr): 3250, 1736, 1677, 1635, 1614, 1601 1564, 1503, 1423, 1271, 1088, 846; δH (400 MHz, $CDCl_3$): 2.59 [3H, *s*, C(3)CH_3], 2.93 [3H, *s*, C(1)CH_3], 2.94 [3H, d, *J* 4.4 Hz, NH(CH_3)], 4.01 [3H, *s*, COO$\underline{CH_3}$], 5.70 [1H, *s*, C(6)H], 6.18 [1H, *bd*, *J* 4.4 Hz, NH]; δ_C (75 MHz, $CDCl_3$): 22.8, 25.9, 29.2, 52.9, 99.7, 120.0, 125.3, 138.3, 149.4, 160.7, 161.0, 169.3, 180.1, 181.3; m/z (ESI^+): 275.3 $(M+H)^+$, 100%; HRMS (ESI^+): Exact mass calculated for $C_{14}H_{15}N_2O_4$ 275.1032. Found 275.1031.

Methyl-1,3-dimethyl-7-((2-morpholinoethyl)amino)-5,8-dioxo-5,8-dihydroisoquinoline-4-carboxylate (5). Amination of methyl 1,3-dimethyl-5,8 dioxo-5,8-dihydroisoquinoline-4-carboxylate (0.151 g, 0.616 mmol) with 4-(2-aminoethyl)morpholine (0.160 g, 1.230 mmol) yielded the product as a bright red solid, (0.171 g, 74%). m.p. 150.0 – 153.0 °C; ν_{max}/cm^{-1} (KBr): 3324, 2947, 2830, 1744, 1672, 1628, 1610, 1496, 1382, 1348, 1320, 1248, 1192, 1118, 1103; δ_H (300 MHz, $CDCl_3$): 2.50 [4H, *t*, *J* 4.5 Hz, N($\underline{CH_2}$) x2], 2.59 [3H, *s*, C(3)CH_3], 2.69 [2H, *t*, *J* 5.9 Hz, CH_2(3')], 2.95 [3H, *s*, C(1)CH_3], 3.21 [2H, *q*, *J* 5.6 Hz, CH_2(2')], 3.76 [4H, *t*, *J* 4.5, O(CH_2) x2], 4.00 [3H, *s*, COO(CH_3)], 5.69 [1H, *s*, C(6)H], 6.72 [1H, *s*, NH]; δ_C (100 MHz, $CDCl_3$): 22.8, 26.0, 38.4, 52.9, 53.1 [2xCH_2], 55.4, 66.8 [2xCH_2], 100.0, 120.1, 125.3, 138.3, 148.4, 160.6, 160.9, 169.4, 180.2, 181.4; m/z (ESI^+): 374.3 $(M+H)^+$, 100%; HRMS (ESI^+): Exact mass calculated for $C_{19}H_{24}N_3O_5$ 374.1716. Found 374.1713. Single crystals were grown from ethanol. Crystals of **(5)** are monoclinic, space group $P2_1/n$, formula $C_{19}H_{23}N_3O_5$, M = 373.40, a = 6.8732(3) Å, b = 16.6383(7) Å, c = 16.3749(7) Å β = 91.7080(10)°, U = 1871.77(14) Å^3, $F(000)$ = 792, m(Mo Ka) = 0.097 mm^{-1}, R_{int} = 0.043, $R(F_o)$ = 0.042, for 3030 observed reflections with I > 2s(I), $wR_2(F^2)$ = 0.124 for all 3863 unique reflections.

Methyl 7-[4-hydroxybutyl)amino]-1,3-dimethyl-5,8-dioxo-5,8-dihydroisoquinoline-4-carboxylate (6). Amination of methyl 1,3-dimethyl-5,8-dioxo-5,8-dihydroisoquinoline-4-carboxylate (0.501 g, 2.043 mmol), with 4-amino-1-butanol (0.350 mL, 4.08 mmol) yielded the product as an orange solid, (0.481 g, 71%). m.p. 103.0 – 105.0 °C; ν_{max}/cm^{-1} (KBr): 3425, 3239, 2951, 1703, 1678, 1628, 1614, 1566, 1515, 1437, 1380, 1329, 1289, 1232, 1205, 1094. 1035; δH (300 MHz, $CDCl_3$): 1.63-1.74 [2H, *m,* NHCH$_2\underline{CH_2}$], 1.76-1.87 [2H, *quin., J* 7.3 Hz, OCH$_2\underline{CH_2}$], 2.59 [3H, *s*, C(3)CH_3], 2.92 [3H, *s*, C(1)CH_3], 3.23 [2H, *q*, *J* 6.5 Hz, OCH_2], 3.72 [2H, *t*, *J* 7.0 Hz (NH)$\underline{CH_2}$], 4.01 [3H, *s*, O(CH_3)], 5.71 [1H, *s*, C(6)H], 6.38 [1H, *bs*, NH]; δ_C (75 MHz, $CDCl_3$): 22.6, 24.7, 26.0, 29.7, 42.5, 53.0, 62.1, 99.7, 120.0, 125.3, 138.3, 148.5, 160.7, 161.0, 169.4, 180.1, 181.4; m/z (ESI^+): 333.2 $(M+H)^+$, 100%; HRMS (ESI^+): Exact mass calculated for $C_{17}H_{21}N_2O_5$ 333.1450. Found 333.1441.

Methyl-7-(benzylamino-1,3-dimethyl-5,8-dioxo-5,8-dihydroisoquinoline-4-carboxylate (7). Amination of methyl 1,3-dimethyl-5,8-dioxo-5,8-dihydroisoquinoline-4-carboxylate (0.301 g, 1.227 mmol) with benzylamine (0.260 mL, 2.473 mmol) yielded the product as a dark orange solid, (0.381 g, 89%). m.p. 165.0 – 167.0 °C; ν_{max}/cm^{-1} (KBr): 3338, 2947, 1728, 1673, 1632, 1609, 1567, 1512, 1276, 1205, 1091, 1077; δH (300 MHz, $CDCl_3$): 2.59 [3H, *s*, C(3)CH_3], 2.93 [3H, *s*, C(1)CH_3], 3.99 [3H, *s*, COO(CH_3)], 4.37 [2H, *d*, *J* 5.7 Hz, NH(CH_2)], 5.76 [1H, *s*, C(6)H], 6.42 [1H, *bs*, NH], 7.24-7.41 [5H, *m*, aromatic]; δ_C (75 MHz, DMSO-d_6): 22.6, 26.0, 45.5, 52.8, 99.6, 121.0, 124.7, 127.6

[3xCH], 128.9 [2xCH], 137.5, 138.2, 149.9, 159.5, 159.9, 168.9, 179.3, 181.7; m/z (ESI$^+$): 351.2 (M+H)$^+$, 100%; HRMS (ESI$^+$): Exact mass calculated for $C_{20}H_{19}N_2O_4$ 351.1345. Found 351.1343.

4-(Methoxycarbonyl)-1,3-dimethyl-7-(methylamino)-5,8-dioxo-5,8-dihydroisoquinoline 2-oxide (12). Amination of methyl 4-(methoxycarbonyl)-1,3-dimethyl-5,8-dioxo-5,8-dihydroisoquinoline 2-oxide (0.201 g, 0.769 mmol) with methylamine (33% solution in absolute ethanol) (15.0 mL, 1.21 mmol) yielded the product as a dark red solid (0.067 g, 30%). m.p. 242.0 – 243.0 °C; ν_{max}/cm^{-1} (KBr): 3260, 1738, 1682, 1635, 1602, 1537, 1504, 1420, 1313, 1067; δH (400 MHz, $CDCl_3$): 2.52 [3H, *s*, C(3)CH_3], 2.94 [3H, *d*, *J* 5.4 Hz, NH$\underline{CH_3}$], 2.98 [3H, *s*, C(1)CH_3], 4.02 [3H, *s*, COO$\underline{CH_3}$], 5.68 [1H, *s*, C(6)H], 6.07 [1H, *bs*, NH]; δ_C (75 MHz, $CDCl_3$): 15.0, 16.3, 29.3, 53.3, 100.0, 123.9, 124.9, 128.3, 149.2, 151.62, 151.65, 167.0, 178.7, 181.0; m/z (ESI$^+$): 291.3 (M+H)$^+$, 100%; HRMS (ESI$^+$): Exact mass calculated for $C_{14}H_{15}N_2O_5$ 291.0981. Found 291.0985.

4-(Methoxycarbonyl)-1,3-dimethyl-7-((2-morpholinoethyl)-amino)-5,8-dihydroisoquinoline 2-oxide (13). Amination of 4-(methoxycarbonyl)-1,3-dimethyl-5,8-dioxo-5,8-dihydroiso-quinoline 2-oxide (0.121 g, 0.463 mmol) with 4-(2-aminoethyl)morpholine (0.132 g, 1.01 mmol) yielded the product as a red solid, (0.114 g, 64 %). m.p. 110.0 – 113.0 °C; ν_{max}/cm^{-1} (KBr): 3336, 2944, 2822, 1733, 1694, 1623, 1313, 1234, 1117, 1060; δ_H (300 MHz, $CDCl_3$): 2.50 [4H, *t*, *J* 4.5 Hz, N$\underline{CH_2}$ x2], 2.52 [3H, *s*, C(3)CH_3], 2.69 [2H, *t*, *J* 6.0 Hz, N$\underline{CH_2}$], 3.00 [3H, *s*, C(1)CH_3], 3.21 [2H, *q*, *J* 5.5 Hz, NH$\underline{CH_2}$], 3.75 [4H, *t*, *J* 4.5 Hz, OCH_2 x2], 4.02 [3H, *s*, COO$\underline{CH_3}$], 5.67 [1H, *s*, C(6)H], 6.65 [1H, *s*, NH]; δ_C (75 MHz, $CDCl_3$): 15.0, 16.3, 38.5, 53.1 [CH_2 x 2], 53.3, 55.3, 66.8 [CH_2 x 2], 100.3, 124.0, 124.9, 128.3, 148.3, 151.5, 151.6, 167.0, 178.7, 181.0; m/z (ESI$^+$): 390.2 (M+H)$^+$, 100%; HRMS (ESI$^+$): Exact mass calculated for $C_{19}H_{22}N_3O_6$ 388.1509. Found 388.1503.

7-((4-Hydroxybutyl)amino)-4-(methoxycarbonyl)-1,3-dimethyl-5,8-dioxo-5,8 dihydroisoquinoline 2-oxide (14). Amination of 4-(methoxycarbonyl) -1,3-dimethyl-5,8-dioxo-5,8-dihydroiso-quinoline 2-oxide (0.302 g, 1.156 mmol) with 4-amino-1-butanol (0.22 mL, 2.31 mmol) yielded the product as an orange solid, (0.126 g, 30 %). m.p. 70.0 – 72.0 °C; ν_{max}/cm^{-1} (KBr): 3373, 2949, 2869, 1737, 1687, 1609, 1541, 1314, 1284, 1230, 1061; δH (300 MHz, $CDCl_3$): 1.69 [2H, *m,* NHCH$_2\underline{CH_2}$], 1.82 [2H, *m*, OCH$_2\underline{CH_2}$], 2.52 [3H, *s*, C(3)CH_3], 2.98 [3H, *s*, C(1)CH_3], 3.23 [2H, *q*, *J* 6.0 Hz, OCH_2], 3.72 [2H, *t*, *J* 5.7 Hz NH$\underline{CH_2}$], 4.02 [3H, *s*, O(CH_3)], 5.70 [1H, *s*, C(6)H], 6.31 [1H, *bs*, NH]; δ_C (75 MHz, $CDCl_3$): 15.0, 16.3, 24.7, 29.6, 42.6, 53.2, 62.0, 100.0, 123.9, 125.0, 128.2, 148.3, 151.61, 151.65, 167.0, 178.7, 181.1; m/z (ESI$^-$): 347.3 (M-H)$^-$, 70%; HRMS (ESI$^+$): Exact mass calculated for $C_{17}H_{21}N_2O_6$ 349.13941. Found 349.1393

7-(Benzylamino)-4-(methoxycarbonyl)-1,3-dimethyl-5,8-dioxo-5,8-dihydroisoquinoline 2-oxide. Amination of 4-(methoxycarbonyl)-1,3-dimethyl-5,8-dioxo-5,8-dihydroiso-quinoline 2-oxide (0.181 g, 0.69 mmol) with benzylamine (0.15 mL, 1.37 mmol) yielded two regioisomeric products: **C(7) regioisomer (15)**: red/orange solid. (0.141 g, 56%). m.p. 160 - 163°C; R/f 0.15 (ethyl acetate: hexane, 1:1); ν_{max}/cm^{-1} (KBr): 3324, 1742, 1692, 1605, 1542, 1511, 1311, 1225, 1064; δH (300 MHz, $CDCl_3$): 2.52 [3H, *s*, C(3)CH_3], 2.99 [3H, *s*, C(1)CH_3], 4.01 [3H, *s*, COO$\underline{CH_3}$], 4.37 [2H, *d*, *J* 5.7 Hz, NH$\underline{CH_2}$], 5.75 [1H, *s*, C(6)H], 6.35 [1H, *bs*, NH], 7.27 – 7.39 [5H, *m*, aromatic]; δ_C (100 MHz, $CDCl_3$): 15.1, 16.3, 47.0, 53.3, 101.1, 123.9, 124.7, 127.6 [CH x 2], 128.3, 128.4, 129.1 [CH x 2], 135.2, 148.0, 151.6, 151.7, 166.9, 178.9, 181.1; m/z (ESI$^+$): 367.3 (M+H)$^+$, 100%; HRMS (ESI$^+$): Exact mass calculated for $C_{20}H_{19}N_2O_5$ 367.1288. Found 367.12911. **C(6) regioisomer (16)**: Orange solid. (0.0144 g, 6%), m.p. 79-80°C; R/f 0.4 (ethyl acetate: hexane, 1:1); ν_{max}/cm^{-1} (NaCl): 3334, 2923, 2852, 1739, 1671, 1616, 1574, 1516, 1453, 1435, 1373, 1315, 1280, 1231, 1143, 1070, 834, 811, 738; δH (300 MHz, $CDCl_3$): 2.48 [3H, *s*, C(3)CH_3], 3.00 [3H, *s*, C(1)CH_3], 4.01 [3H, *s*, COO$\underline{CH_3}$], 4.34 [2H, *d*, *J* 5.7 Hz, NH$\underline{CH_2}$], 5.79 [1H, *s*, C(6)H], 6.02 [1H, *bs*, NH], 7.24 – 7.41 [5H, *m*, aromatic]; δ_C (75 MHz, $CDCl_3$): 14.7, 15.9, 46.8, 53.3, 103.7, 127.6 [CH x 2], 128.3, 129.1 [CH x 2], 135.4, 146.2, 166.7, 179.1, 182.4; m/z (ESI$^+$): 367.3 (M+H)$^+$, 60%; HRMS (ESI$^+$): Exact mass calculated for $C_{20}H_{18}N_2O_5$ 367.1288. Found 367.1287.

Typical Bromination Procedure

Aminated isoquinolinequinone (1 equivalent) was dissolved in methanol (15 mL). *N*-Bromosuccinimide (2 equivalents) was added portionwise over 1 minute with stirring. The reaction mixture was stirred for 1 hour at room temperature. TLC (100% ethyl acetate) was used to monitor reaction progress. After stirring, the solvent was removed under reduced pressure and was subjected to flash column chromatography (ethyl acetate: hexane). The isolated product was dried overnight under reduced pressure.

Methyl 6-bromo-1,3-dimethyl-7-(methylamino)-5,8-dioxo-5,8-dihydroisoquinoline-4-carboxylate (8). Methyl 1,3-dimethyl-7-(methylamino)-5,8-dioxo-5,8-dihydroisoquinoline-4-carboxylate (0.152 g, 0.554 mmol) was brominated with *N*-bromosuccinimide (0.131 g, 0.736 mmol) yielding the product as a dark red solid (0.125 g, 64%). m.p. 218.0 – 220.0 °C; ν_{max}/cm^{-1} (KBr): 3351, 1733, 1669, 1595, 1572, 1516, 1210, 1088; δH (400 MHz, $CDCl_3$): 2.59 [3H, *s*, C(3)CH_3], 2.91 [3H, *s*, C(1)CH_3], 3.47 [3H, *d*, *J* 5.6 Hz, NH$\underline{CH_3}$], 4.03 [3H, *s*, COO$\underline{CH_3}$], 6.48 [1H, *bs*, NH];]; δ_C (100 MHz, $CDCl_3$): 22.9, 26.0, 29.5, 53.1, 119.2, 125.6, 136.7, 136.8, 151.8, 161.05, 161.18, 168.8, 177.7, 179.6; m/z (ESI$^+$): 353.0 (M+H)$^+$, 5%, 355.0 (M+H)$^+$, 5%; HRMS (ESI$^+$): Exact mass calculated for $C_{14}H_{14}N_2O_4Br$ 353.0137. Found 353.0123.

Methyl-6-bromo-1,3-dimethyl-7-((2-morpholinoethyl)-amino)-5,8-dioxo-5,8-dihydroisoquinoline-4-carboxylate (9). Methyl-1,3-dimethyl-7-((2-morpholinoethyl)amino)-5,8-dioxo-5,8-dihydroisoquinoline-4-carboxylate (0.305 g, 0.817 mmol) was brominated with *N*-bromosuccinimide (0.314 g, 1.764 mmol) yielding the product as a bright red solid, (0.208 g, 56%). m.p. 195.0 – 196.0 °C; ν_{max}/cm^{-1} (KBr): 3193, 2963, 1730, 1682, 1585, 1559, 1328, 1289, 1204, 1116, 1068; δH (300 MHz, $CDCl_3$): 2.54 [4H, *bt*, N$\underline{CH_2}$)x2], 2.58 [3H, *s*, C(3)CH_3], 2.68 [2H, *t*, *J* 5.9 Hz, NHCH$_2\underline{CH_2}$], 2.91 [3H, *s*, C(1)CH_3], 3.77 [4H, *t*, *J* 4.2 Hz, O(CH_2) x2)], 3.97 [2H, *bq*, *J* 5.2 Hz, NH$\underline{CH_2}$], 4.03 [3H, *s*, OCH_3], 7.28 [1H, *bs*, NH]; δ_C (75 MHz, $CDCl_3$): 22.8, 26.0, 41.1, 52.8, 53.1 [2C], 56.3, 66.8 [2C], 119.5, 123.1, 125.5, 136.7, 146.2, 160.90, 160.92, 168.8, 179.8, 183.1; m/z (ESI$^+$): 452.1 (M+H)$^+$, 90%, 454.1 (M+H)$^+$, 100%; HRMS (ESI$^+$): Exact mass calculated for $C_{19}H_{23}N_3O_5Br^{79}$ 452.0821. Found 452.0803.

Methyl-6-bromo-7-[(4-hydroxybutyl)amino]-1,3-dimethyl-5,8-dioxo-5,8-dihydro-isoquinoline-4-carboxylate (10). Methyl-7-[(4-hydroxybutyl)amino]-1,3-dimethyl-5,8-dioxo-5,8-dihydroisoquinoline-4-carboxylate (0.152 g, 0.457 mmol) was brominated with *N*-bromosuccinimide (0.091 g, 0.511 mmol) yielding the product as a dark orange solid, (0.14 g, 75%). m.p. 153.0 – 155.0 °C; ν_{max}/cm^{-1} (KBr): 3538, 3281, 2926, 2878, 1721, 1681, 1591, 1567, 1333, 1203, 1094; δH (300 MHz, $CDCl_3$): 1.68 [2H, *m,* $NHCH_2\underline{CH_2}$], 1.82 [2H, *m*, $OCH_2\underline{CH_2}$], 2.58 [3H, *s*, $C(3)CH_3$], 2.90 [3H, *s*, $C(1)CH_3$], 3.73 [2H, *t*, *J* 6.0 Hz $NH\underline{CH_2}$], 3.94 [2H, *q*, *J* 6.7 Hz, OCH_2], 4.02 [3H, *s*, OCH_3], 6.55 [1H, *bs*, NH], 8.1 [1H, *bs*, OH]; δ_C (75 MHz, $CDCl_3$): 22.8, 25.9, 27.3, 29.3, 29.5, 53.1, 62.1, 125.6, 125.8, 131.4, 136.8, 144.7, 161.0, 161.1, 168.8, 177.2, 179.8; m/z (ESI^+): 411.1 $(M+H)^+$, 90%, 413.0 $(M+H)^+$, 100%; HRMS (ESI^+): Exact mass calculated for $C_{17}H_{20}N_2O_5Br^{79}$ 411.0556. Found 411.0541.

Methyl 7-(benzylamino)-6-bromo-1,3-dimethyl-5,8-dioxo-5,8-dihydroisoquinoline-4-carboxylate (11). Methyl 7-(benzylamino-1,3-dimethyl-5,8-dioxo-5,8-dihydroisoquinoline-4-carboxylate (0.122 g, 0.348 mmol) was brominated with *N*-bromosuccinimide (0.063 g, 0.354 mmol) yielding the product as a red solid, (0.102 g, 70%). m.p. 154.0 – 155.0 °C; ν_{max}/cm^{-1} (KBr): 3344, 3023, 2954, 2921, 1732, 1677, 1588, 1566, 1400, 1331, 1196, 1180; δH (300 MHz, $CDCl_3$): 2.59 [3H, *s*, $C(3)CH_3$], 2.88 [3H, *s*, $C(1)CH_3$], 4.03 [3H, *s*, $O(CH_3)$], 5.08 [2H, *d*, *J* 5.8 Hz, $NH\underline{CH_2}$], 6.47 [1H, *bs*, NH], 7.29 – 7.44 [5H, *m*, Ar-H]; δ_C (75 MHz, $CDCl_3$): 22.9, 25.9, 49.4, 53.1, 125.6, 127.7 [2C], 128.3, 129.1 [2C], 131.3, 136.6, 137.1, 139.3, 148.2, 161.0, 161.1, 168.6, 179.6, 180.0; m/z (ESI^+): 429.1 $(M+H)^+$, 90%, 431.1 $(M+H)^+$, 100%; HRMS (ESI^+): Exact mass calculated for $C_{20}H_{18}N_2O_4Br^{79}$ 429.0450 Found 429.0445

Electrochemical Measurements

Cyclic voltammetry (CV) and square wave voltammetry (SWV) measurements of compounds **2**, **3**, **11**, **15**, **16** were performed at room temperature using a CHI1040 A electrochemical workstation (CH Instrument, Austin, USA). The electrochemical cell consists of a Pt working electrode (diameter of 2 mm, IJ Cambria Scientific Ltd, UK), a Pt wire counter electrode (Sigma-Aldrich, Dublin, Ireland), and non-aqueous reference electrode (Ag/Ag^+, BASi Analytical Instruments, West Lafayette, IN). A 0.1 M solution of tetrabutylammonium tetrafluoroborate in acetonitrile (ACN) was used as supporting electrolyte. The Pt electrode was polished using diamond slurry (1 µm) with wet MasterTex paper, followed by sonication in deionized water for 5 min. The CVs were run in the potential range 0.0 to -1.2 V *versus* non-aqueous Ag/Ag^+ and used to estimate half-wave potential $E_{1/2}$. Well-defined quasi-reversible waves were observed for the compounds, the cathodic peak related to the reduction of quinone, and the anodic one due to its re-oxidation. The first half-wave potential values, $E^I_{1/2}$ evaluated from the voltammograms obtained at a scan rate of 100 mVs^{-1}. SWVs were used for double confirmation; amplitude (E_{sw}) of 25 mV, a potential increment (ΔE) of 4 mV and a frequency (f) of 5 Hz. Stock solutions (5 mM) were prepared in ACN before use and working solutions were prepared by dilution of stock solution with the supporting electrolyte; 2 mM each of **2**, **3**, **7**, and **15** and 3 mM of **16**.

Cancer Cell Growth Assays (NCI60 Screening)

One-dose study: Tested compounds were initially solubilised in DMSO, diluted into RPMI 1640 and 5% fetal bovine serum/L-glutamine, and added to 96-well plates containing cell lines previously cultured for 24 h. After 48-h incubation, the media were removed, and the cells were fixed and stained with sulforhodamine B to determine overall percent growth/total protein content. Unbound dye was removed with five washes of 1% acetic acid, and the plates were allowed to air dry. The dye was then resolubilised in Tris buffer, and the colorimetric absorbance was measured (515 nm). Growth inhibition was measured relative to the response generated from proliferating cells cultured under identical conditions for 48 hrs. Data from one-dose experiments pertains to the percentage growth at 10 µM.

Five-dose study: Serial 5 x 10-fold dilution from an initial DMSO stock solution was performed, prior to incubation at each individual concentration (10 nM, 100 nM, 1 µM, 10 µM and 100 µM). Using seven absorbance measurements (time zero (Tz), control growth (C), and test growth in the presence of drug at the five concentration levels (Ti)), the percentage growth was calculated at each of the drug concentrations levels. Percentage growth inhibition was calculated as: [(Ti-Tz)/(C-Tz)] x 100 for concentrations for which Ti ≥ Tz, [(Ti-Tz)/Tz] x 100 for concentrations for which Ti < Tz. Three dose response parameters were calculated for each experimental agent. Growth inhibition of 50% (GI_{50}) was calculated from [(Ti-Tz)/(C-Tz)] x 100 = 50, which is the drug concentration resulting in a 50% reduction in the net protein increase (as measured by Sulforhodamine B staining) in control cells during the drug incubation. The drug concentration resulting in total growth inhibition (TGI) was calculated from Ti = Tz. The LC_{50} (concentration of drug resulting in a 50% reduction in the measured protein at the end of the drug treatment as compared to that at the beginning) indicating a net loss of cells following treatment was calculated from [(Ti-Tz)/Tz] x 100 = -50. Values were calculated for each of these three parameters if the level of activity was reached; however, if the effect was not reached or was exceeded, the value for that parameter was expressed as greater or less than the maximum or minimum concentration tested.[46,47]

COMPARE analysis

COMPARE analysis was conducted using the private access system provided by the National Cancer Institute (https://dtp.cancer.gov/databases_tools/compare.htm). Seed compounds were analysed using a number of target sets: synthetic compounds, BEC referral set, mechanistic set, standard agents, marketed drugs and diversity set. While the minimum correlation was set to 0.4, correlations of less than 0.65 were discounted. All other criteria were unchanged. The top 2-4 correlations between all target sets were chosen. Experiments that were carried out at different concentrations to the seed compound were ignored unless the concentration

deviated by ±0.1. COMPARE analysis was conducted solely on five dose data for compounds **3**, **15** and **16**.[48] GI_{50} correlation between **15** and **16** was conducted using the 'matrix compare' function.

Adduct Binding Study

Sample preparation: Quinones **2**, **3**, **7**, **11**, **15**, **16** were dissolved in acetonitrile to make 2 mM solution individually (solution A). The biological nucleophiles (cysteine, glutathione and serine) were dissolved in water/methanol (1:1) resulting in a 3mM solution individually (Solution B).

Reaction Conditions: 50 µL of solution A, 50 µL of solution B and 0.9 mL of methanol were added to a HPLC vial and the HPLC vial was placed into a water bath at 37°C for 12 hours. The resulting mixture was qualitatively screened using LC/MS (see SI) for the identification of the adducts. In all cases mono-adduct formation was observed. See supplementary information for full adduct binding study procedure.

Conclusions

In summary, a new IQQ *N*-oxide framework **3** was developed which exhibited outstanding activity against the NCI60 panel of human tumour cell lines. We report the first single crystal X-ray structure confirmation of the C(7) amination of the IQQ seed **2**, which had been previously been characterised with 2D-NMR methods. Through the generation of fourteen novel IQQ's divided into three series (amino IQQs, brominated IQQ's and IQQ *N*-oxides) it was revealed that the amino IQQ's exhibited the poorest effects on cell growth at 10 µM concentration, however, upon substitution of the 6-position with bromine we observe a significant increase in cytotoxicity by 32% on average. As predicted by electrochemical studies, if bromine is removed and a *N*-oxide moiety is installed we observe equipotent activity between both series.

Employing cyclic voltammetry, we identified IQQ *N*-oxide **16** as the most electropositive species in the benzylamine series, whereas benzylamine IQQ **7** the least electropositive. This data suggests a correlation exists between the increase in redox potential to an increase in cytotoxicity, indicating the electronic nature of the quinone moiety plays a role in the biological mechanism of action, a common trend for quinone based anticancer agents. Adduct formation studies revealed that IQQ frameworks **2** and **3** covalently bind to oxygen and sulfur based biological nucleophiles *in vitro*, but, once aminated with benzylamine, only sulfur based adducts were isolated.

The benzylamine analogues **11**, **15** and **16** were the most potent of the IQQ *N*-oxide series and were selected for five-dose NCI screening. The most potent analogue identified was the C(6) benzylamine IQQ N-oxide **16**, a compound isolated as a minor product and exhibited nM GI50 values against 31/57 human tumour cell lines screened as part of the NCI60 panel. The most responsive cancers identified being ovarian, melanoma, breast and colon. IQQ *N*-oxide **16** is a promising lead for future structure activity relationship studies and exhibits an activity of 535 nM against the doxorubicin resistant tumour cell line NCI/ADR-RES.

Conflicts of interest

The authors confirm that there are no conflicts to declare.

Acknowledgements

The authors would like to acknowledge the Irish Research Council for funding this research and the National Cancer Institute (NCI) screening program for 60-cell line testing. This article is based upon work from COST Action CA15135, supported by COST.

Author Contributions: RDK performed the research in relation to the synthesis and characterization on novel compounds. AB/JDG performed the electrochemical research. UBRK/SEL performed the crystallography studies. RDK/FOM designed the research and drafted the manuscript; all authors reviewed the draft manuscript

References

1 J. L. Bolton, T. Dunlap, *Chem. Res. Toxicol*., 2017, **30**, 13-37.
2 I. Klopčič, M. S. Dolenc, *Chem. Res. Toxicol*., 2019, **32**, 1-34.
3 D. J. Milanowski, K. R. Gustafson, J. A. Kelley, J. B. McMahon, *J. Nat. Prod*., 2004, **67**, 70-73.
4 U. W. Hawas, M. Shaaban, K. A. Shaaban, M. Speitling, A. Maier, G. Kelter, H. H. Fiebig, M. Meiners, E. Helmke, H. Laatsch, *J. Nat. Prod*., 2009, **72**, 2120-2124.
5 S. Kuang, G. Liu, R. Cao, L. Zhang, Q. Yu, C. Sun, *Oncotarget*, 2017, **8**, 104057-104071.
6 J. Wang, Y. Jing, *Canc. Biol. Ther.,* 2008, **7**, 1875-1884.
7 M. Brisson, C. Foster, P. Wipf, B. Joo, R. J. Tomko, Jr., T. Nguyen, J. S. Lazo, *Mol. Pharmacol*., 2007, **71**, 184-192
8 K. Kristjansdottir, J. Rudolph, *Chemistry and Biology*, 2004, **11**, 1043-1051.
9 L. Pu, A. A. Amoscato, M. E. Bier, J. S. Lazo, *J. Biol. Chem*., 2002, **277**, 46877-46885.
10 J. S. Lazo, D. C. Aslan, E. C. Southwick, K. A. Cooley, A. P. Ducruet, B. Joo, A. Vogt, P. Wipf, *J. Med. Chem*., 2001, **44**, 4042-4049.
11 A. K. Brenner, H. Reikvam, A. Lavecchia, Ø. Bruserud., *Molecules*, 2014, **19**, 18414-18447.
12 C. F. Thorn, C. Oshiro, S. Marsh, T. Hernandez-Boussard, H. McLeod, T. E. Klein, R. B. Altman, *Pharmacogenetics and Genomics*, 2011, **21**, 440-446.
13 A. A. Fisher, M. T. Labenski, S. Malladi, V. Gokhale, M. E. Bowen, R. S. Milleron, S. B. Bratton, T. J. Monks, S. S. Lau, *Biochemistry*, 2007, **46**, 11090-11100.
14 A. Begleiter, G. W. Blair, *Cancer Research*, 1984, **44**, 78-82.
15 V. Delgado, A. Ibacache, V. Arancibia, C. Theoduloz, J. A. Valderrama, *Molecules*, 2013, **18**, 721-734.
16 V. Delgado, A. Ibacache, C. Theoduloz and J. A. Valderrama, *Molecules*, 2012, **17**, 7042-7056.
17 J. A. Ibacache, J. A. Valderrama, V. Arancibia, C. Theoduloz, G. G. Muccioli, J. Benites, *J. Chil. Chem. Soc*., 2016, **61**, 3191-3194.
18 J. A. Ibacache, V. Delgado, J. Benites, C. Theoduloz, V. Arancibia, G. G. Muccioli, J. A. Valderrama, *Molecules*, 2014, **19**, 726-739.
19 J. A. Valderrama, V. Delgado, S. Sepúlveda, J. Benites, C. Theoduloz, P. B. Calderon, G. G. Muccioli, *Molecules*, 2016, **21**, 1199-1213.
20 J. A. Valderrama, J. A. Ibacache, V. Arancibia, J. Rodriguez, C. Theoduloz, *Bioorg. Med. Chem*., 2009, **17**, 2894-2901.

21 J. A. Valderrama., M. F. González, D. Mahana-Pessoa, R. A. Tapia, H. Fillion., F. Pautet., J. A. Rodriguez, C. Theoduloz., G. Schmeda-Hirschmann, *Bioorg. Med. Chem*., 2006, **14**, 5003-5011.
22 J. A. Ibacache, J. Faundes, M. Montoya, S. Mejias, J. A. Valderrama, *Molecules*, 2018, **23**, 439-449.
23 H. Ni, C. Xia, Y. Zhao, *Med. Chem. Res*., 2017, **26**, 2861-2869.
24 F. R. F. Dias, J. S. Novais, T. A. do Nascimento Santos Devillart, W. A. da Silva, M. O. Ferreira, R. de S. Loureiro, V. R. Campos, V. F. Ferreira, M. C. B. V. de Souza, H. C. Castro, A. C. Cunha, *Eur. J. Med. Chem*., 2018, **156**, 1-12.
25 G. Bertuzzi, S. Crotti , P. Calandro, B. F. Bonini, I. Monaco, E. Locatelli, M. Fochi, P. Zani, E. Strocchi, A. Mazzanti, M. Chiariello, M. C. Franchini, *Chem. Med. Chem*., 2018, **13**, 1744-1750.
26 C.K. Ryu, A. L. Song, J. A. Hong, *Bioorg. Med. Chem. Lett*., 2013, **23**, 2065-2068.
27 V. M. Dembitsky, T. A. Gloriozova, V. V. Poroikov, *Phytomedicine*, 2015, **22**, 183-202.
28 B. M. Ramalingam, N. D. Moorthy, S. R. Chowdhury, T. Mageshwaran, E. Vellaichamy, S. Saha, K. Ganesan, B. N. Rajesh, S. Iqbal, H. K. Majumder, K. Gunasekaran, R. Siva, A. K. Mohanakrishnan, *J. Med. Chem*., 2018, **61**, 1285-1315.
29 A. M. Mfuh, O. V. Larionov, *Curr. Med. Chem*., 2015, **22**, 2819-2857.
30 S. B. Reddy, S. K. Williamson, *Expert Opin. Investig. Drugs*, 2009, **18**, 77-87.
31 T. Fryatt, H. I. Pettersson, W. T. Gardipee, K. C. Bray, S. J. Green, A. M. Z. Slawin, H. D. Beallb, C. J. Moody, *Bioorg. Med. Chem*., 2004, **12**, 1667-1687.
32 E. Lengvel, J. E. Burdette, H. A. Kenny, D. Matei, J. Pilrose, P. Haluska, K. P. Nephew, D. B. Hales, M. S. Stack, *Oncogene*, 2014, **33**, 3619-3633.
33 R. Vang, le-M. Shih, R. J. Kurman, *Adv. Anat. Pathol*., 2009, **1**, 267-282.
34 L. A. Garraway, H. R. Widlund, M. A. Rubin, G. Getz, A. J. Berger, S. Ramaswamy, R. Beroukhim, D. A. Milner, S. R. Granter, J. Du, C. Lee, S. N. Wagner, C. Li, T. R. Golub, D. L. Rimm, M. L. Meyerson, D. E. Fisher, W. R. Sellers, *Nature*, 2005, **436**, 117-122.
35 S. Sangthong, H. Ha, T. Teerawattananon, N. Ngamrojanavanich, N. Neamati, N. Muangsin, *Bioorg. Med. Chem. Lett.,* 2013, **23**, 6156-6160.
36 O. N. Ikediobi, H. Davies, G. Bignell, S. Edkins, C. Stevens, S. O'Meara, T. Santarius, T. Avis, S. Barthorpe, L. Brackenbury, G. Buck, A. Butler, J. Clements, J. Cole, E. Dicks, S. Forbes, K. Gray, K. Halliday, R. Harrison, K. Hills, J. Hinton, C. Hunter, A. Jenkinson, D. Jones, V. Kosmidou, R. Lugg, A. Menzies, T. Mironenko, A. Parker, J. Perry, K. Raine, D. Richardson, R. Shepherd, A. Small, R. Smith, H. Solomon, P. Stephens, J. Teague, C. Tofts, J. Varian, T. Webb, S. West, S. Widaa, A. Yates, W. Reinhold, J. N. Weinstein, M. R. Stratton, P. A. Futreal, R. Wooster, *Mol. Cancer. Ther.,* 2006, **5**, 2606-2612.
37 M. J. Duffy, N. C. Synnott, J. Crown, *Eur. J. Cancer*, 2017, **83**, 258-265.
38 T. Robak, E. Lech-Maranda, A. Korycka, E. Robak, *Curr. Med. Chem*., 2006, **13**, 3165-3189.
39 M. K. Kharel, P. Pahari, M. D. Shepherd, N. Tibrewal, S. E. Nybo, K. A. Shaaban, J. Rohr, *Nat. Prod. Rep*., 2012, **29**, 264-325.
40 Y. Wang, M. A. Islam, R. A. David, S. R. McAlpine, *Bioorg. Med. Chem. Lett*., 2015, **25**, 249-253.
41 J. Zhang, Y. Liu, D. Shi, G. Hu, B. Zhang, X. Li, R. Liu, X. Han, X. Yao, J. Fang, *Eur. J. Med. Chem*., 2017, **10**, 435-447.
42 J. Kim, E. K. Lee, S. J. Park, N. D. Kim, D. Hyun, C. G. Lee, J. H. Lee, K. M. Yang, K. Heo, T. G. Son, *Int. J. Oncol*., 2012, **40**, 157-162.
43 C. F. C. Lam, M. M. Cadelis, B. R. Copp, *Tetrahedron*, 2017, **73**, 4779-4785.
44 G. M. Sheldrick, *Acta Crystallogr., Sect. C: Struct. Chem*., 2015, **71**, 3-8.
45 C. F. Macrae, I. J. Bruno, J. A. Chisholm, P. R. Edgington, P. McCabe, E. Pidcock, L. Rodriguez-Monge, R. Taylor, J. van de Streek, P. A. Wood, *J. Appl. Crystallogr*., 2008, **41**, 466-470.
46 National Cancer Institute. Developmental Therapeutics Program. NCI-60 Human Tumour Cell Lines Screen. Available online: https://dtp.cancer.gov/discovery_development/nci-60/default.htm (accessed on 08 August 2019)
47 R. H. Shoemaker, *Nat. Rev. Cancer,* 2006, **6**, 813–823.
48 K. D. Paull, R. H. Shoemaker, L. Hodes, A. Monks, D. A. Scudiero, L. Rubinstein, J. Plowman, M. R. Boyd, *J. Natl. Cancer Inst*. 1989, **81**, 1088–1092.